JYX
JYVÄSKYLÄN YLIOPISTO
UNIVERSITY OF JYVÄSKYLÄ

This is a self-archived version of an original article. This version may differ from the original in pagination and typographic details.

Author(s): AL-Rjoub, A.; Costa, P.; Rebouta, L.; Radović, I. Bogdanović; Arstila, Kai; Barradas, N.P.; Alves, E.; Matilainen, A.; Pischow, K.

Title: A study of solar thermal absorber stack based on CrAlSiNx/CrAlSiNxOy structure by ion beams

Year: 2019

Version: Accepted version (Final draft)

Copyright: © 2019 Elsevier BV

Rights: CC BY-NC-ND 4.0

Rights url: https://creativecommons.org/licenses/by-nc-nd/4.0/

Please cite the original version:

AL-Rjoub, A., Costa, P., Rebouta, L., Radović, I. B., Arstila, K., Barradas, N.P., Alves, E., Matilainen, A., & Pischow, K. (2019). A study of solar thermal absorber stack based on CrAlSiNx/CrAlSiNxOy structure by ion beams. Nuclear Instruments and Methods in Physics Research Section B: Beam Interactions with Materials and Atoms, 450, 195-199. https://doi.org/10.1016/j.nimb.2018.04.024

A study of solar thermal absorber stack based on $CrAlSiN_x$ /$CrAlSiN_xO_y$ structure by ion beams

A. AL-Rjoub[1], P. Costa[1], L. Rebouta[1], I. Bogdanović Radović[2], K. Arstila[3], N.P. Barradas[4], E. Alves[5,*], A. Matilainen[6], K. Pischow[6]

[1]Center of Physics, University of Minho, Campus de Azurém, 4800-058 Guimarães, Portugal

[2]Ruđer Bošković Institute, Zagreb, Croatia

[3]University of Jyvaskyla, Department of Physics, P.O. Box 35, FI-40014 University of Jyvaskyla, Finland

[4]Centro de Ciências e Tecnologias Nucleares, IST, Universidade de Lisboa, Bobadela, Portugal

[5]Instituto de Plasmas e Fusão Nuclear, IST, Universidade de Lisboa, Lisboa, Portugal

[6]Savo Solar Oy, Insinöörinkatu 7, 50100 Mikkeli, Finland

* Corresponding author: ealves@ctn.tecnico.ulisboa.pt

Abstract

Renewable energies are foreseen as a major energy resource for next generations. Among several energy sources and technologies available, Concentrated Solar Power (CSP) technology has a great potential, but it needs to be optimised, in particular to reduce the costs, with an increase of the operating temperature and long term stability. This goal can be achieved by tailoring the composition and multilayer structure of films. In this work we present and discuss the results obtained from solar absorber coatings based on nitride/oxynitride structures. A four-layer film structure, W/CrAlSiNx(HA)/CrAlSiNxOy(LA)/SiAlOx, was deposited on stainless steel substrates using magnetron sputtering deposition method. Simulations were performed to establish the best spectral properties of the multilayer stacks with optical constants of single layers and film thickness. The elemental analysis was performed using Rutherford Backscattering Spectrometry (RBS) and Time of flight Elastic Recoil Detection Analysis (TOF-ERDA). To assess the thermal stability of the coatings the samples were thermal annealed at 400°C, in air, and at 600°C, in vacuum. The results obtained by RBS and TOF-ERDA reveal good oxidation resistance and thermal stability. Also, the optical measurements confirm the potential of these materials for the use in CSP technology.

Keywords: solar selective absorber, Rutherford Backscattering Spectrometry (RBS), Time of flight Elastic Recoil Detection Analysis (TOF-ERDA), $CrAlSiN_x$ /$CrAlSiN_xO_y$, sputtering

1. Introduction

Concentrated solar power (CSP) technology for electricity production and other applications uses parabolic-trough solar systems, that concentrate sunlight up to 80 times onto evacuated receiver tubes. These tubes contain some improved coated selective layers that are responsible for the absorption of solar thermal radiation. Resulting energy can be subsequently used in steam turbines to produce electricity [1][2][3]. However, comparing with other resources, the relative cost of electricity generated by solar thermal technology is still high. The cost can be reduced by improving the optical and thermal properties of the coating materials, increasing the operating temperature more than 450 ºC [4] and by improvements of the long-term stability. Improvements can be done by an adequate materials selection [5], maintaining the optical performance at higher temperatures and with higher durability. Efficient designs should have high absorbance (α) at solar radiation region (wavelength range of 0.3- 2.0 μm), low thermal emittance in infrared (IR) region (wavelength range greater 2.0 μm) and long-term resistance against oxidation and barrier diffusion at high temperature.

Usually, the absorbers are multilayers coating that consist of IR-reflective metallic base layer such as tungsten or molybdenum, a double interference absorption (high absorber (HA) and low absorber (LA)) layers and a ceramic anti-reflection (AR) surface layer [6][7][8]. One of the main causes for optical degradation of the coating is surface oxidation due to the penetration of oxygen into the coating - substrate interface, through pinholes, which cause a change in the optical properties and oxidation of the nitride and back reflector layers . On the other hand, the metal atoms of the substrate may diffuse through the coating, which causes degradation of the optical properties and deterioration of coating adhesion.

Rutherford Backscattering Spectrometry (RBS) and Time of flight Elastic Recoil Detection Analysis (TOF-ERDA) can be used as effective techniques to study the elemental depth profiles, chemical composition and stability issues of such these coatings, since those techniques depend on the atomic number and mass of elements, which make the analysis more efficient than other techniques [9]. For example, there are a lot of challenges and difficulties in studying thermal stabilities and elemental diffusion between stacks layers. Moreover, using RBS and TOF-ERDA is main challenge, due to the thicknesses of the multilayers of stacks, e.g. in this study, if tungsten layer thicker than 200 nm, then RBS analysis will fail to distinguish between chromium (Cr) and tungsten (W) in the spectra. In this paper, we present and discuss the results obtained from solar absorber coatings based on W/CrAlSiNx(HA)/ CrAlSiNxOy(LA)/SiAlOx, which

were deposited on stainless steel substrates using the magnetron sputtering deposition method. The chemical composition and depth profiles were determined using RBS and TOF-ERDA, with the aim of understanding the oxidation, diffusion of metallic elements and thermal stability issues of such these designs

2. Experimental

The layers of the optical stack were deposited by dc magnetron sputtering with following conditions: P_{Ar}=0.37 Pa, current density 6.4 mA/cm^2, pulsed bias of -60 V, f =90 kHz, room temperature and base pressure 2×10^{-4} Pa, (for tungsten layer the current density was 12.7 mA/cm^2). The stainless steel substrates AISI304 (25 mm× 25 mm × 0.7 mm) were ultra sound cleaned in acetone for 15 min, and were subjected into ion etching for 15 min. For stack simulation, individual layers of $CrAlSiN_x$ and $CrAlSiN_xO_y$ were deposited on glass substrates (38 mm × 26 mm×0.95 mm) with different nitrogen and oxygen partial pressures for 1 min. Then, spectrophotometry measurements (Shimadzu PC3100 spectrophotometer), in the wavelength range of 0.25 – 2.5 μm, were used to measure the transmittance and the reflectance of the layers. The reflectance data were corrected according to the Al -reference reflectance curve. Results were used to simulate the optical constants and thicknesses of the optical stack using SCOUT software [10]. The final multilayer stack was deposited on stainless steel substrates with experimental details shown in Table I. Then, the stacks were annealed in air at 400 ºC for 650 h and in vacuum at 600 ºC for 50 h and 650h respectively. Normal solar absorptance (α_s) and thermal emittance were determined using the procedure described in [11].

Thick $CrAlSiN_x$ and $CrAlSiN_xO_y$ layers were deposited on and Si mirror polished substrates. As already mentioned, the chemical composition of stack (as deposited, after air and vacuum annealing) was determined by using RBS and TOF-ERDA measurements. RBS was performed at the CTN/IST Van de Graaff accelerator using 2 MeV $^4He^+$ beam and detectors at 140º and 165º to the beam direction. Normal incidence was used in the experiments and the obtained data were analysed with the IBA Data Furnace NDF [12]. Atomic composition and depth profiles of all elements present in the sample were determined using TOF-ERDA which is described in detail in [13]. TOF-ERDA measurements were performed using 6 MV Tandem Van de Graaff accelerator located at Ruđer Bošković Institute. For the measurements 20 MeV $^{127}I^{6+}$ ions with 20° incidence angle toward the sample surface and TOF-ERDA spectrometer positioned at angle

of 37.5° toward the beam direction were used. Analysis of TOF-ERDA spectra was done using program Potku [14] and MCERD [15].

Table I: The experimental details of th multilayer stack.

Layer	**Target**[1]	**Deposition time**	**Target Current density(A/cm^2)**	**P_{Ar} (Pa)**	**Reactive gas partial pressure (Pa)**[2]
W	W	2 min & 30 s	12.7	0.37	-
$CrAlSiN_x$	Cr-Al (70-30 at%)and 9 Si pellets	1 min & 27 s	6.4	0.37	$P_{N2} = 0.051$
$CrAlSiO_yN_x$	Cr-Al (70-30 at%) and 9 Si pellets	46 s	6.4	0.37	$P_{O2/N2} = 0.068$
$SiAlO_x$	Si-Al (80-20 at%)	1 min & 38 s	6.4	0.37	$P_{O2} = 0.062$

[1]The diameter of the targets :W, Cr-Al and Si-Al is 10 cm, and the diameter of Si pellets is 1cm, and placed on the Cr-Al target erosion zone.

[2] P_{N2}, $P_{N2/O2}$ and P_{O2} are the nitrogen, nitrogen/oxygen (85%:15%), and oxygen partial pressures of reactive gases, respectively.

3. Results and discussion

3.1 Design of the multilayer

Fig. 1 shows a scheme of the theoretical stack designed by SCOUT software using optical constants of individual thin layers that were deposited on glass substrates. SCOUT allows the calculation of the spectral optical constants, refractive index (n) and extinction coefficient (κ), besides the thickness of each individual layer.

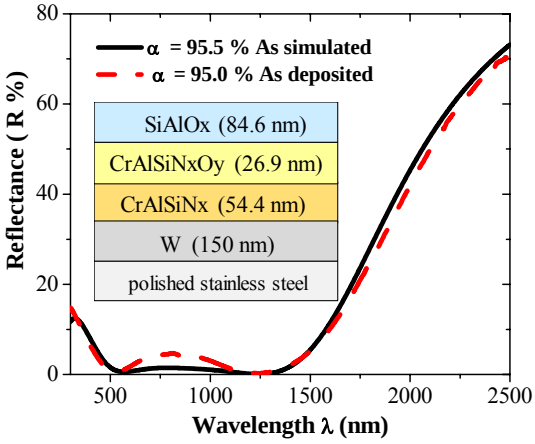

Fig. 1- Schematic diagram of the simulated thicknesses of each layer of the optical stack as obtained by SCOUT, in addition to the simulated and experimental reflectance curves of the absorber design.

Total simulated thickness of the whole multilayer (W/CrAlSiN$_x$ /CrAlSiN$_x$O$_y$ /SiAlO$_x$) is ~ 316 nm. W layer shows a typical morphology of a columnar growth type, and it is polycrystalline as also confirmed by X-ray diffraction (XRD), as already reported [11]. Remaining layers are amorphous and reveal a featureless morphology as shown by single layers studied previously[16]. The final design shows simultaneously high solar absorbance in average α= 95.2 % and low emissivity ε= 9.8 % (calculated for 400 ºC).

3.2 Thermal stability

Selective absorber stack should be thermally stable and should show high oxidation resistance for a long lifetime. Thus, annealing tests in air at 400 ºC and in vacuum at 600 ºC for 650h were performed to study the thermal stability and the oxidation resistance of the stack. Fig. 2 represents the reflectance curves of as deposited stacks and stacks after annealing, respectively. From those results it can be concluded that the optical stack is showing a good thermal stability, except the existence of a very small shift in the step of the reflectance curve towards lower wavelength for the vacuum annealed case. These changes were seen after the first vacuum annealing step (50 h) but no significant further changes were found with subsequent anneling steps until 650 h. As a result, the values of solar absorptance and emittance show a very small variation due to that shift. Small changes after annealing can be related to the oxidation of some Si atoms, or it can be related to the diffusion of layer elements (such as the diffusion of Cr

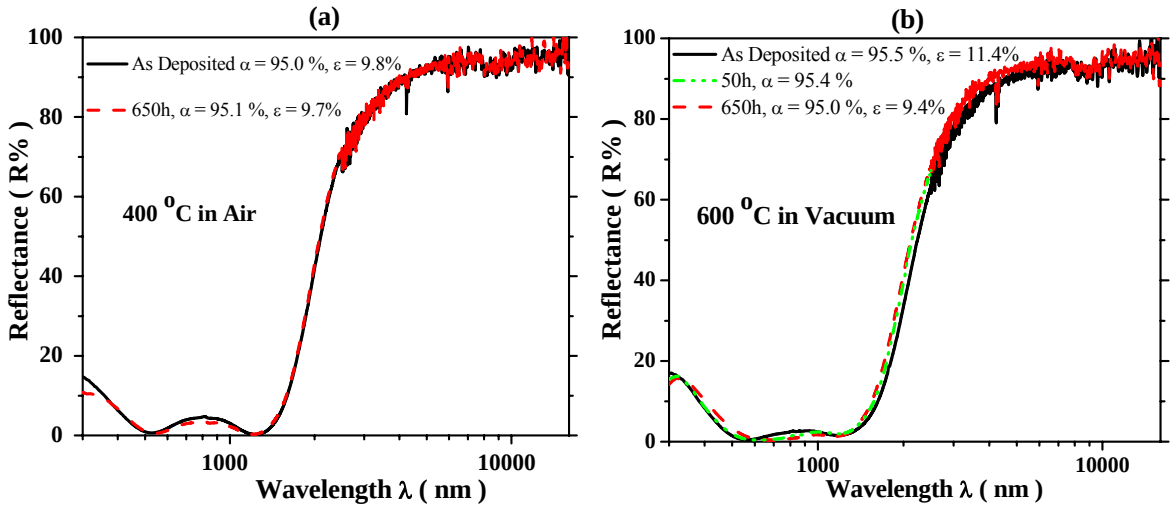

Fig. 2- Reflectance of as deposited optical stack and after (a) air thermal annealing at 400 ºC and (b) vacuum thermal annealing at 600 ºC, with measured value of thermal absorptance (α) and thermal emittance (ε) (calculated for 400 ºC).

towards surface as can be concluded by RBS and TOF-ERDA analyses). Fig.3 shows two RBS spectra of thick $CrAlSiN_x$ and $CrAlSiN_xO_y$ single layers, prepared with same partial pressure as those used in multilayer.

The front edge positions of different elements are correlated with the relative concentrations of the different elements. It is difficult to distinguish between silicon and aluminum due to the small difference in their atomic masses, and the (Al+Si)/Cr composition ratio was determined for both samples and it was 2.0. With the used conditions, the separation between Al and Si front edges is very small and the Si/Al composition ratio was determined by TOF-ERDA, as shown in the next section**.**

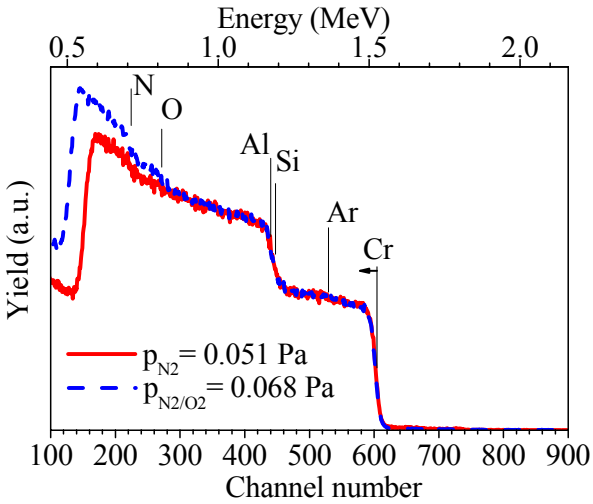

Fig. 3- RBS spectra (with 140° scattering angle) of thick $CrAlSiN_x$ (1.3 µm) and $CrAlSiN_xO_y$ (1.2 µm) single layers, prepared with same partial pressure as those used in multilayer. (P_{N2} , $P_{N2/O2}$ are the nitrogen and nitrogen/oxygen (85%/15%) partial pressures during the deposition of nitride and oxynitride, respectively).

Fig. 4 shows RBS spectra of three optical stacks deposited in the same run and subjected to different thermal loads, namely as deposited, after air annealing at 400 ºC for 650 h and after vacuum annealing at 600 ºC for 650 h. The positions of different elements, located at the sample surface, are indicated on the graph. The analysis shows only a small difference between the as deposited and annealed samples, which indicates good thermal stability of the stack. After air annealing a small change is seen between channel numbers 150 and 350, which was not clearly identified, and seems to be in the stainless steel substrate because was not possible to fit it to the deposited layers.,. After vacuum annealing at 600 ºC, it can be seen that changes occur in the W and Cr depth profiles, which are in accordance with the diffusion of small amount of tungsten towards the stainless steel substrate and chromium towards the surface. The $CrAlSiN_x$ and

$CrAlSiN_xO_y$ layers are substoichiometric in terms of (N+O)/(Cr+Al+Si) atomic ratio [16], which means that some of Cr atoms are in metallic oxidation state [16], because Cr are less reactive than Al and Si, and can diffuse towards the surface. The substoichiometry of those layers are due to required optical properties of HA and LA layers. The general evaluation shows that no other significant changes occurred after annealing in vacuum and air. So, a diffusion barrier layer should be added between stainless steel substrate and tungsten layer to reduce diffusion between these layers. In order to avoid the Cr diffusion it will be necessary to change the (Al+Si)/Cr ratio. This is related with the possibility to get the same optical properties of two absorbing layers, but having $CrAlSiN_x$ and $CrAlSiN_xO_y$ layers stoichiometric in terms of (N+O)/(Cr+Al+Si) atomic ratio, because they would be more chemically stable and would have better diffusion barrier properties.

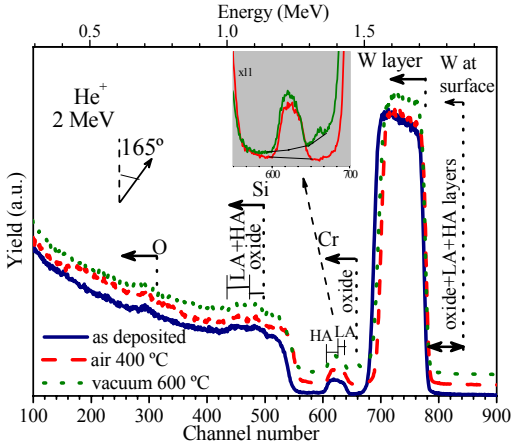

Fig. 4- RBS spectra (with 165° scattering angle) of the as deposited stack, after air annealing at 400 ºC and vacuum annealing at 600 ºC, both for 650 h. Figure legend shows a magnified spectra of after air and vacuum annealing with linear background, which emphasizes the presence of Cr on the sample surface from the stack after vacuum annealing.

TOF-ERDA measurements allowed to determine the concentration depth profiles of all the elements in the three samples. Monte Carlo (MC) simulations [15] were used to find the best fits between the elemental energy spectra extracted from TOF-ERDA measured data and the simulated energy spectra taking in the account all the details of the experimental setup and the multiple scattering effects in the recoiling process. Fig.5 shows an example of TOF-ERDA histogram data, experimental and simulated energy spectra for oxygen recoils and the corresponding depth profiles used in the simulations. All the observed elements (H, C, N, O, Al, Si, Cr, Ar, W, and Fe) were fitted with simulations in the same way, yielding the concentration

profiles of all the elements in the three samples. The oxygen and chromium depth profiles allow the identification of the three outermost layers, $SiAlO_x$, $CrAlSiN_xO_y$ and $CrAlSiN_x$, as indicated in the Fig. 6. A small amount of Cr is also seen at the sample surface after the annealing in vacuum (Fig. 6 bottom), which is in accordance with results obtained by RBS. In the as deposited samples the (Al+Si)/Cr composition ratio is 1.3 for oxynitride layer and 1.7 for nitride layer. These values increased in the annealed samples, being more significant in the vacuum annealed samples, which increased to 1.6 and 2.1, respectively. These values correspond to a small decrease of Cr content in both layers, which suggests the Cr atoms at surface diffused from nitride and oxynitride layer. The amount of Cr atoms at the surface corresponds to 5.6% of all Cr atoms in the annealed sample. The Si/Al ratio in oxide layer, is 2.0 in average, and 0.5 and 0.8 oxynitride and nitride layers, respectively. The difference in Si/Al and (Al+Si)/Cr composition ratios in oxynitride and nitride layers is mainly due to the effect of target poisoning, because those layers were deposited with different nitrogen and oxygen partial pressures, being higher in oxynitride layer. This reduces the sputtering rate of different elements and this effect is higher for Al and Si when compared to Cr, because Al and Si are more reactive than Cr. The consequence is the reduction of the (Al+Si)/Cr composition ratio when passing from nitride to oxynitride. However, this difference was not seen in RBS analysis of thick single layers (Fig.3), which would be sensitive to such a reduction. The RBS data of the stack samples (Fig. 4), however, is not very sensitive to the (Al+Si)/Cr ratio, because this layer is thin and not at the surface. The TOF-ERDA composition results for that ratio were used in the fits shown in Fig. 4, showing consistency of the two sets of data.

Small differences in the thicknesses of the layers were found, which can be due the positioning of the samples during the deposition. Hydrogen, carbon, and argon were observed as impurities in the three absorber layers (see fig 5). Their atomic concentrations were below 3% in all the layers in all the samples. Hydrogen and argon concentrations decreased significantly in the annealing treatments.

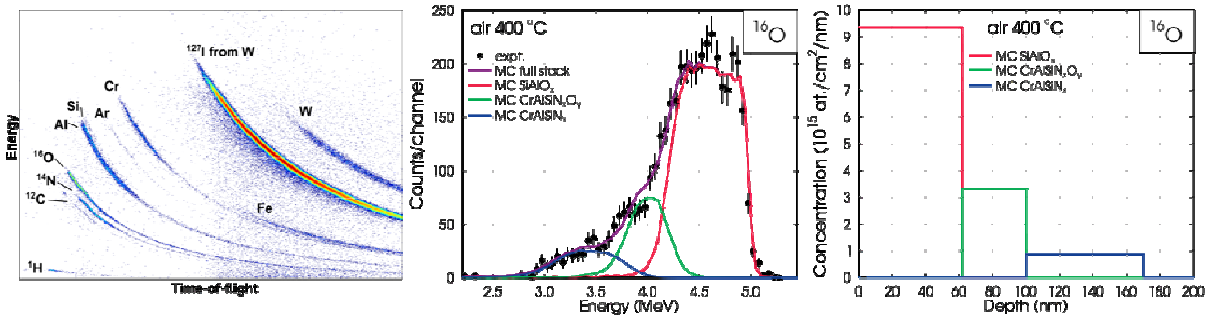

Fig. 5 - ToF–E histogram (on the left) for the measurement of a sample annealed in air at 400 °C, experimental oxygen energy spectrum (in the middle) extracted from the measurement data and the MC simulated energy spectrum with contributions from the three absorber layers, and (on the right) the concentration profiles used in the MC simulations.

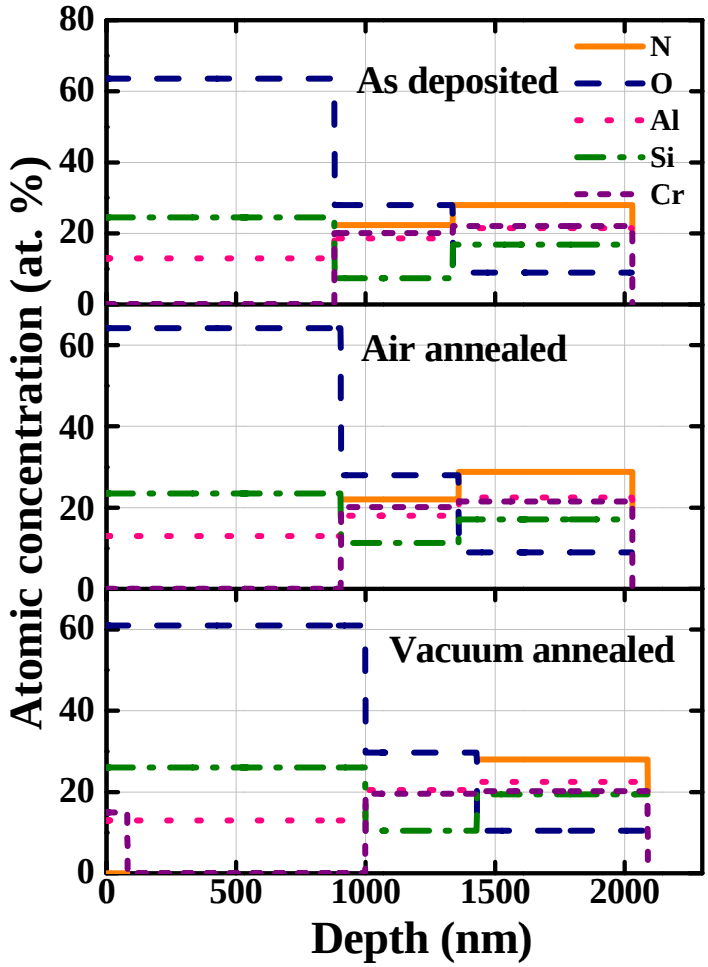

Fig. 6 - Elemental depth profiles determined from the TOF-ERDA measurements with MC simulations: as deposited stack (top), after air annealing at 400 ºC (middle) and after vacuum annealing at 600 ºC (bottom), both for 650 h.

4. Conclusions

Magnetron sputtering method was used to fabricate solar thermal absorber stack, which can be used for high temperature applications. The designed structure was simulated by the SCOUT software, that is a multilayer of four structural layers (W/CrAlSiN$_x$ /CrAlSiN$_x$O$_y$ /SiAlO$_x$), as back reflector/ high absorber/ low absorber/antireflector layers, respectively. Experimental design shows simultaneously high average solar absorbance α=95.2% and low emissivity ε= 9.8% (at 400 ºC) together with the high thermal stability during annealing in air at 400 ºC and in vacuum at 600 ºC for 650 h. RBS and TOF-ERDA analyses were efficiently used to obtain the chemical composition and elemental depth profile of the solar thermal absorber stack. Measurements have shown that a small amount of W diffused during annealing toward stainless steel substrate, and at the same time Cr diffused from the nitride and oxynitride layers toward the surface. The reason is certainly the substoichiometry of those layers in terms of (N+O)/(Cr+Al+Si) atomic ratio. Thus, those layers have part of the Cr atoms in metallic oxidation state, which favours the diffusion. Optical changes were seen after the first vacuum annealing step (50 h) but no significant further changes were found with subsequent anneling steps until 650 h, which suggests that this Cr diffusion can be limited to those Cr atoms in the lower oxidation state. In order to minimize the W diffusion to add a diffusion barrier layer between the stainless steel substrate and the tungsten layer will be necessary. On the other hand, to avoid the Cr diffusion it will be necessary to increase the stoichiometry of CrAlSiN$_x$ and CrAlSiN$_x$O$_y$ layers while maintaining their optical properties.

ACKNOWLEDGMENTS

The authors acknowledge the support of FCT in the framework of the Strategic Funding UID/FIS/04650/2013 and the financial support of FCT, POCI and PORL operational programs through the project POCI-01-0145-FEDER-016907 (PTDC/CTM-ENE/2882/2014), co-financed by European community fund FEDER. K. Arstila acknowledges the support by Academy of Finland Center of Excellence in Nuclear and Accelerator Based Physics (Ref. 251353).

References

[1] A. Fernández-García, E. Zarza, L. Valenzuela, M. Pérez, Parabolic-trough solar collectors and their applications, Renew. Sustain. Energy Rev. 14 (2010) 1695–1721.

doi:10.1016/j.rser.2010.03.012.
[2] S.D. Odeh, G.L. Morrison, M. Behnia, Modelling of parabolic trough direct steam generation solar collectors, 62 (1998) 395–406.
[3] J. Ward, Modelling, optimisation and performance evaluation of a parabolic trough solar collector steam generation system, Sol. Energy. 60 (1997) 49–59.
[4] L. Rebouta, A. Sousa, M. Andritschky, F. Cerqueira, C.J. Tavares, P. Santilli, K. Pischow, Solar selective absorbing coatings based on AlSiN/AlSiON/AlSiOy layers, Appl. Surf. Sci. 356 (2015) 203–212. doi:10.1016/j.apsusc.2015.07.193.
[5] C.E. Kennedy, Review of Mid- to High- Temperature Solar Selective Absorber Materials, NREL/TP-520-31267, Natl. Renew. Energy Lab. Goledn, CO. (2002).
[6] L. Rebouta, A. Sousa, P. Capela, M. Andritschky, P. Santilli, A. Matilainen, K. Pischow, N.P. Barradas, E. Alves, Solar selective absorbers based on Al2O3:W cermets and AlSiN/AlSiON layers, Sol. Energy Mater. Sol. Cells. 137 (2015) 93–100. doi:10.1016/j.solmat.2015.01.029.
[7] C. Zou, W. Xie, L. Shao, Functional multi-layer solar spectral selective absorbing coatings of AlCrSiN/AlCrSiON/AlCrO for high temperature applications, Sol. Energy Mater. Sol. Cells. 153 (2016) 9–17. doi:10.1016/j.solmat.2016.04.007.
[8] A. Dan, K. Chattopadhyay, H.C. Barshilia, B. Basu, Angular solar absorptance and thermal stability of W / WAlN / WAlON / Al 2 O 3 -based solar selective absorber coating, Appl. Therm. Eng. 109 (2016) 997–1002. doi:10.1016/j.applthermaleng.2016.04.069.
[9] N.P. Barradas, C. Jeynes, Advanced physics and algorithms in the IBA DataFurnace, Nucl. Instruments Methods Phys. Res. Sect. B Beam Interact. with Mater. Atoms. 266 (2008) 1875–1879. doi:10.1016/j.nimb.2007.10.044.
[10] W. Theiss, SCOUT Thin Film Analysis Software Handbook, (2002).
[11] D. Dias, L. Rebouta, P. Costa, A. Al-rjoub, M. Benelmeki, C.J. Tavares, N.P. Barradas, E. Alves, P. Santilli, K. Pischow, Optical and structural analysis of solar selective absorbing coatings based on AlSiO x□: W cermets, Sol. Energy. 150 (2017) 335–344. doi:10.1016/j.solener.2017.04.055.
[12] N.P. Barradas, C. Jeynes, Advanced physics and algorithms in the IBA DataFurnace, Nucl. Instruments Methods Phys. Res. Sect. B Beam Interact. with Mater. Atoms. 266 (2008) 1875–1879. doi:10.1016/j.nimb.2007.10.044.
[13] Z. Siketic, I. Bogdanovic, M. Jaks, Development of a time-of-flight spectrometer at the Ruđer Bošković Institute in Zagreb, Nucl. Instruments Methods Phys. Res. B. 266 (2008) 1328–1332. doi:10.1016/j.nimb.2007.12.070.
[14] K. Arstila, J. Julin, M.I. Laitinen, J. Aalto, T. Konu, S. Karkkainen, S. Rahkonen, M. Raunio, J. Itkonen, J.-P. Santanen, T. Tuovinen, T. Sajavaara, Potku – New Analysis Software for Heavy Ion Elastic Recoil Detection Analysis K. Detection Analysis, Nucl. Inst. Methods Phys. Res. B. 331 (2014) 34–41. doi:10.1016/j.nimb.2014.02.016.
[15] K. Arstila, T. Sajavaara, J. Keinonen, Monte Carlo simulation of multiple and plural scattering in elastic recoil detection, Nucl. Inst. Methods Phys. Res. B. 174 (2001) 163–172.
[16] A. Al-Rjoub, P. Costa, L. Rebouta, M.F. Cerqueira, P. Alpuim, N.P. Barradas, E. Alves, Characterization of magnetron sputtered sub-stoichiometric CrAlSiNx and CrAlSiOyNx coatings, Surf. Coat. Technol. 328 (2017) 134–141. doi:10.1016/j.surfcoat.2017.08.038.